Electronic Supplementary Material (ESI) for Materials Advances.

Supporting Information

Enhancing the Sensitivity of a Water Stable MOF as a H_2S Gas Sensor by the Fabrication of Mixed-Matrix Membrane

Mouli Das Dawn, [a] Karabi Nath, [a] Subhajit Saha [a], Pritam Kumar Roy, [b] Mahitosh Mandal [b] and Kumar Biradha*, [a]

[a] Department of Chemistry, Indian Institute of Technology Kharagpur, Kharagpur 721302, India

*E-mail: kbiradha@chem.iitkgp.ac.in

Fax: +91-3222- 282252. Tel.: +91-3222-283346.

[b] School of Medical Science and Technology, Indian Institute of Technology, Kharagpur 721302, India

Contents

General aspects:

All the chemicals and solvents such as Fumaric acid, 3-picolyl amine, triphenyl phosphite, Sodium sulfide, $Zn(NO_3)_2 \cdot 6H_2O$, Polyvinylpyrrolidone, Poly(vinylidene fluoride) pyridine, and DMF were purchased from local chemical suppliers and used without purification. The XRPD patterns were recorded with a BRUKER-AXS-D8-ADVANCE diffractometer at room temperature. The diffuse reflectance spectra (DRS) were recorded with a Cary model 5000 UV−vis−near-infrared (NIR) spectrophotometer. The solid-state luminescence spectra were collected with a Spex Fluorolog-3 (model FL3-22) spectrofluorimeter. FTIR spectra were recorded with a PerkinElmer Instrument spectrum Rx Serial No. 73713. The TGA data had been recorded with a PerkinElmer instrument, Pyris Diamond TG/DTA under a nitrogen atmosphere at a heating rate of 10 °C/min. Field-emission scanning electron microscopy (FESEM) was performed on a ZEISS VP 300 instrument with an Oxford EDS detector, operated at an accelerating voltage of 5−10 kV. The solution state luminescence spectra were collected with a Shimadzu RF-6000 spectrofluorophotometer. The solution state absorbance spectra were recorded with the use of a Shimadzu (model no. UV2450) UV–vis spectrophotometer. Fluorescence lifetimes were measured using a time-correlated single photon counting (TCSPC) spectrometer of IBH (U.K.). X-ray photoelectron spectroscopy (XPS) was performed in an ESCALAB Xi, Thermo-Scientific, UK, having a monochromatic Al Kα X-ray source (1486.6 eV). The CAE (constant analyzer energy) for survey spectra is 100 eV and that for high-resolution spectra is 50 eV.

Synthesis and Experimental methods:

Section S1: Synthesis of Ligand (**BP3YF**):

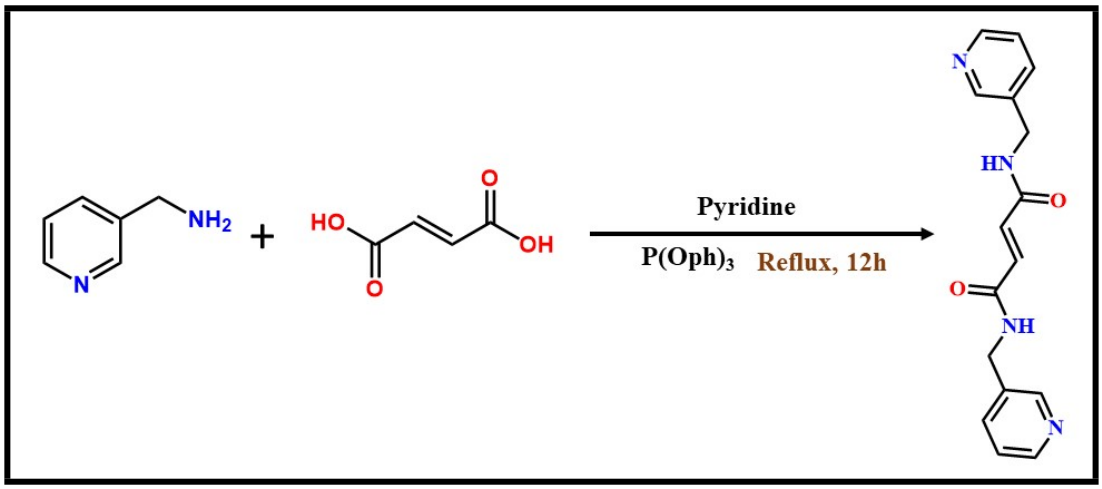

Scheme S1 (**BP3YF**)

Ligand BP3YF was prepared by following the reported procedure. [S1]

^{1}H-NMR spectrum of 3-PAFA in d_6-DMSO

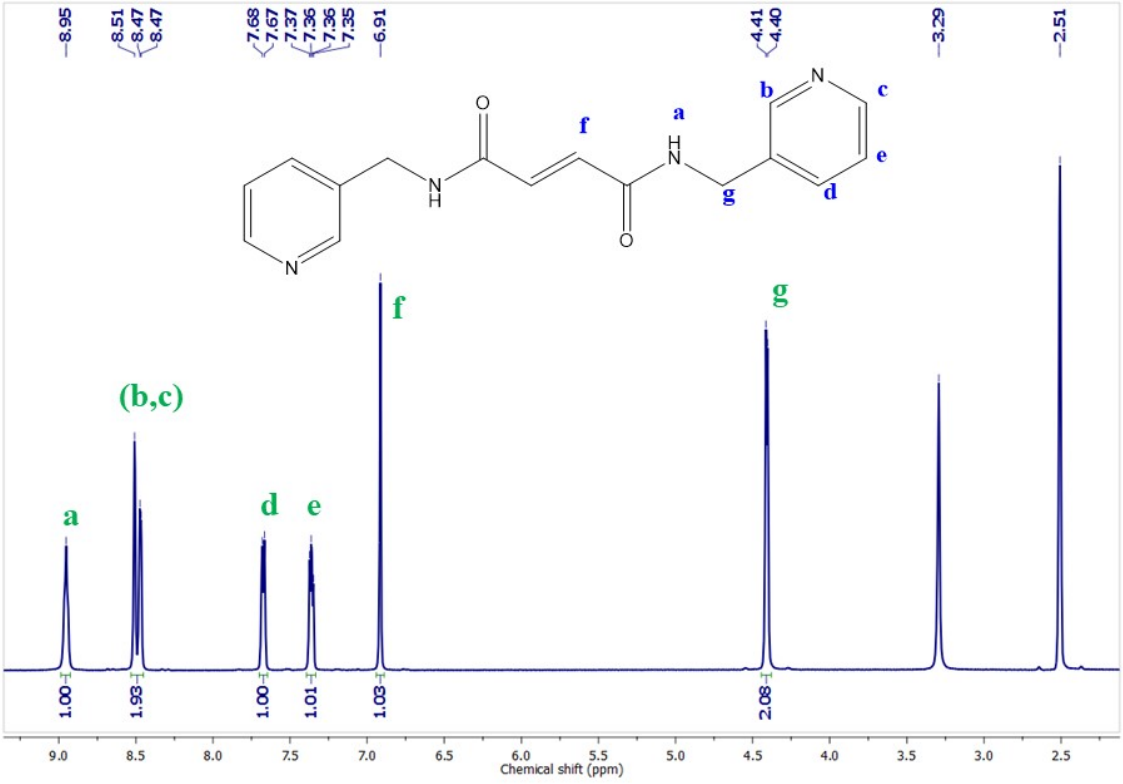

Section S2: Synthesis of MOFs (**Zn-cpb**, **Zn-bdc** and **Zn-btc**)

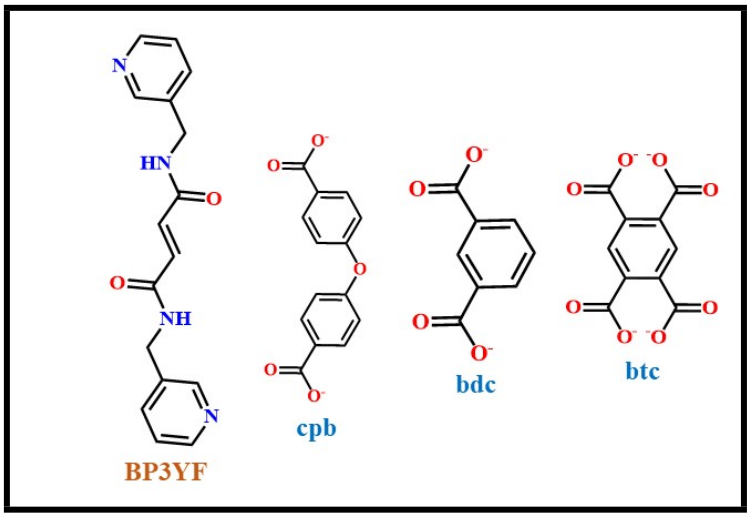

Scheme S2. Chemical structures of ligand and ancillary ligands.

1. Synthesis of **Zn-cpb**: $\{[Zn(BP3YF)(cpb)]\}_n$

A mixture of **BP3YF** (29.6 mg, 0.1 mmol), sodium oxybisbenzoate (14mg, 0.1 mmol) and $Zn(NO_3)_2$ (29.7 mg, 0.1 mmol) were taken in a sealed glass tube along with 8 ml of DMF-water. The mixture was heated at 100 °C for 2 days and slowly cooled to room temperature. Colorless block shaped crystals of **Zn-cpb** were obtained, which were then washed with water several times and dried in air. Yield: 68%. Elemental anal. Calcd for $C_{30}H_{24}N_4O_7Zn$ (%): C, 58.31; H, 3.91; N, 9.07. Obsd (%): C, 58.52; H, 3.64; N, 8.67.

2. Synthesis of **Zn-bdc**: $\{[Zn(BP3YF)(bdc)]\}_n$

A mixture of **BP3YF** (29.6 mg, 0.1 mmol), sodium isophthalate (10 mg, 0.1 mmol) and $Zn(NO_3)_2$ (29.7 mg, 0.1 mmol) was taken in a sealed glass tube along with 8 ml of DMF-water. The mixture was heated at 100 °C for 2 days and plate shaped crystals of **Zn-bdc** appeared upon slow cooling to room temperature. The crystals were washed properly with water and dried in air. Yield: 72%. Elemental anal. Calcd for $C_{24}H_{20}N_4O_6Zn$ (%): C, 54.82; H, 3.83; N, 10.65. Obsd (%): C, 53.96; H, 3.80; N, 10.58.

3. Synthesis of **Zn-btc**: $\{[Zn_2(BP3YF)(btc)(H_2O)_2]\}_n$

A mixture of **BP3YF** (29.6 mg, 0.1 mmol), sodium pyromellitate (15 mg, 0.1 mmol) and $Zn(NO_3)_2$ (29.7 mg, 0.1 mmol) were taken in a sealed glass tube along with 8 ml of DMF-water. The mixture was heated at 100 °C for 2 days and slowly cooled to room temperature. The crystals were washed properly with water and dried in air. Yield: 72%. Elemental anal.

Calcd for $C_{13}H_{11}N_2O_6Zn$ (%): C, 43.81; H, 3.11; N, 7.86. Obsd (%): C, 43.62; H, 3.03; N, 7.94.

Section S3

Membrane Preparation

In this study, the composite membranes were fabricated by a slurry-casting method. The microcrystalline powder of **Zn-bdc** was mixed with PVDF for the corresponding composite membrane, and the amount of **Zn-bdc** was 0, 20, 40, and 60 wt % in membranes **Zn-bdc_0@PVDF**, **Zn-bdc_20@PVDF**, **Zn-bdc_40@PVDF**, and **Zn-bdc_60@PVDF** respectively. A similar procedure was utilized for the preparation of all composite membranes; in a typical preparation process of **Zn-bdc_60@PVDF**, 60 mg of **Zn-bdc** microcrystals were ultrasonically dispersed in DMF (4 mL) for 30 min to produce a suspension, PVDF powders were added to the suspension, and the mixture was stirred at room temperature for 45 min to obtain a homogeneous jelly. This homogeneous jelly was poured onto a petri-dish, which was dried at 100 °C for 8 h to remove DMF. The solidified membrane was removed from the petri-dish, washed with deionized water, and dried at 120 °C under vacuum to eliminate residual solvent prior to further experimental measurements.

Section S4: Pertinent crystallographic parameters of MOFs

Crystal Structure Determination. All the single-crystal data were collected on a Bruker-APEX-II CCD X-ray diffractometer using graphite monochromated Mo Kα radiation (λ = 0.71073 Å) at room temperature (100 K), by the hemisphere method. The structures were solved by direct methods and refined by least-squares methods on F^2 using SHELX-2014.[50] Nonhydrogen atoms were refined anisotropically, and hydrogen atoms were fixed at calculated positions and refined using a riding model. The H atoms attached to the O atom or N atoms are located wherever possible and refined using the riding model.

Table S1

Crystallographic parameters of Zn-cpb, Zn-bdc and Zn-btc

Compound (CCDC No.)	Zn-btc (2282228)	Zn-cpb (2282229)	Zn-bdc (2282230)
Formula	$C_{13}H_{11}N_2O_6Zn$	$C_{30}H_{24}N_4O_7Zn$	$C_{24}H_{20}N_4O_6Zn$
MW	356.38	617.92	525.83
Temperature (K)	293(2)	293(2)	302(2)
Crystal system	Triclinic	Triclinic	Monoclinic
Space group	P-1	P-1	P21/c
a (Å)	6.139(5)	10.7634(2)	13.130(4)
b (Å)	8.638(2)	11.1742(2)	10.419(3)
c (Å)	12.092(3)	12.6382(2)	16.247(5)
α (deg)	84.001(7)	78.282(4)	90
β (deg)	84.561(8)	69.923(4)	90.526(11)
γ (deg)	87.900(7)	82.799(4)	90
V (Å^3)	634.6(3)	1395.3(3)	2222.52
Z	2	2	4
d (g/cm^3)	1.866	1.471	1.571
F(000)	358	632	1072
Crystal size/mm^3	0.4 x 0.39 x 0.40	0.26 x 0.2 x 0.08	0.3 x 0.29 x 0.25
Radiation	MoK\α	MoK\α	MoK\α
Index ranges	-6<=h<=7, -10<=k<=11 -15<=l<=14	-15<=h<=15, -15<=k<=15 -15<=l<=18	-16<=h<=15, -12<=k<=12 -19<=l<=20
2Θ range for data collection	1.70º to 26.98º	1.74º to 31.03º	2.32º to 25.99º
μ(mm^{-1})	1.970	0.935	1.156
Reflections collected	7654	18844	23442
Independent reflections	2654	7265	4155
Data/restraints/parameters	2654/0/205	7265/0/379	4155/2/316
Goodness-of-fit on F^2	0.941	2.181	1.750
R_1 (I>2σ(I))	0.0377	0.0744	0.132
Final R indexes [all data] wR2 (all data)	0.1124	0.1494	0.3141
Largest diff. peak and hole	1.292 and -0.632 e.Å^{-3}	2.751 and -0.702 e.Å^{-3}	1.631 and -0.947 e.Å^{-3}

Table S2

Bond Distances (Å) and Bond Angles (°) for Zn-cpb, Zn-bdc, and Zn-btc.

Zn-cpb		Zn-bdc		Zn-btc	
Bond	**Distance (Å)**	**Bond**	**Distance (Å)**	**Bond**	**Distance (Å)**
Zn1-O1A	1.992(4)	Zn1-O3A	1.945(7)	Zn1-O3	2.080(4)
Zn1-O1B	2.536(4)	Zn1-O1A	1.953(6)	Zn1-O9	2.078(4)
Zn1-O2B	1.972(5)	Zn1-N11A	2.056(8)	Zn1-N1	2.070(4)
Zn1-N11A	2.056(7)	Zn1-N21A	2.075(8)	Zn1-O5	2.003(4)
Zn1-N11B	2.069(5)			Zn1-O6	2.010(4)
Bonds	**Angle(°)**	**Bonds**	**Angle(°)**	**Bonds**	**Angle(°)**
O1A-Zn1-N11A	101.8(2)	O3A-Zn1-N11A	113.5(3)	O3 Zn1 O9	169.4(1)
O1A-Zn1-N11B	94.6(2)	O3A-Zn1-O1A	94.4(3)	O3 Zn1 N1	102.8(1)
O1A-Zn1-O1B	168.4(2)	O3A-Zn1-N21A	114.4(3)	O3 Zn1 O5	85.3(1)
O1A-Zn1-O2B	111.4(2)	N11A-Zn1-O1A	116.8(3)	O3 Zn1 O6	87.1(1)
N11A-Zn1-N11B	102.7(2)	N11A-Zn1-N21A	102.6(3)	O9 Zn1 N1	87.4(1)
N11A-Zn1-O1B	85.8(2)	O1A-Zn1-N21A	115.8(3)	O9 Zn1 O5	87.5(1)
N11A-Zn1-O2B	124.7(2)			O9 Zn1 O6	94.8(1)
N11B-Zn1-O1B	92.1(2)			N1 Zn1 O5	115.9(1)
N11B-Zn1-O2B	116.6(2)			N1 Zn1 O6	97.2(1)
O1B-Zn1-O2B	57.1(2)			O5 Zn1 O6	146.9(1)
N11B-Zn1-O1A	94.6(2)			O6 Zn1 N1	97.2(1)
				O5 Zn1 N1	115.9(1)

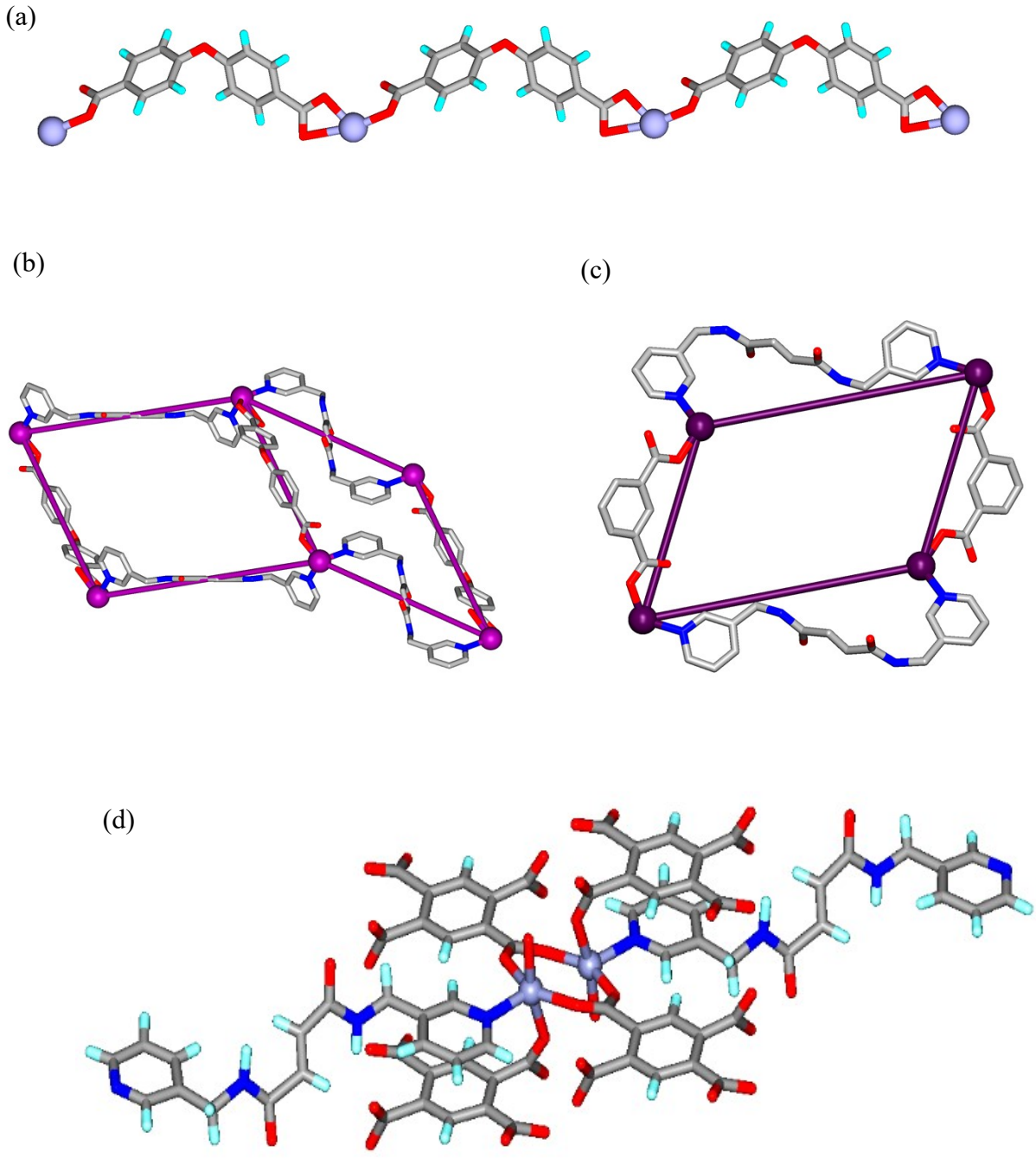

Figure S1 Illustrations for the crystal structure of **Zn-cpb, Zn-bdc** and **Zn-btc**: a) Coordination environment around the central metal ion Zn(II) in **Zn-cpb** (b) Formation of rectangular and square cavities through **BP3YF** and **cpb** moieties (c) Formation of rectangular cavities through **BP3YF** and **bdc** moieties (d) Distorted trigonal bipyramidal geometry around Zn(II) in **Zn-btc.**

Section S5: IR spectra of **Zn-cpb, Zn-bdc** and **Zn-btc**

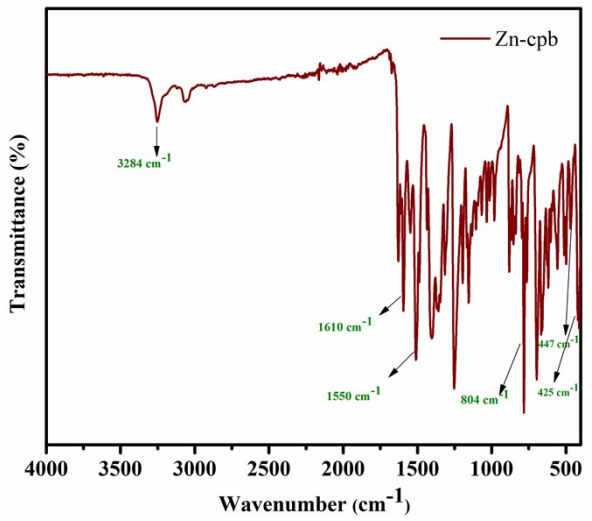

Figure S2: IR spectrum of Zn-cpb: 3284 (N-H stretch),1610 (amide C=O stretch), 1550(amide II), 804 cm^{-1} (Zn-O symmetric stretching), 447 cm^{-1} (Zn-O symmetric stretching), 425 cm^{-1} (Zn-N symmetric stretching)

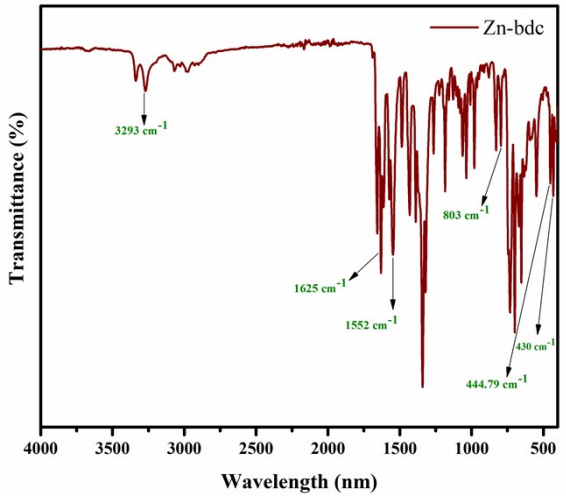

Figure S3: IR spectrum of Zn-bdc: 3293 (N-H stretch),1625 (amide C=O stretch), 1552(amide II), 803 cm^{-1} (Zn-O symmetric stretching), 444.79 cm^{-1} (Zn-O symmetric stretching), 430 cm^{-1} (Zn-N symmetric stretching)

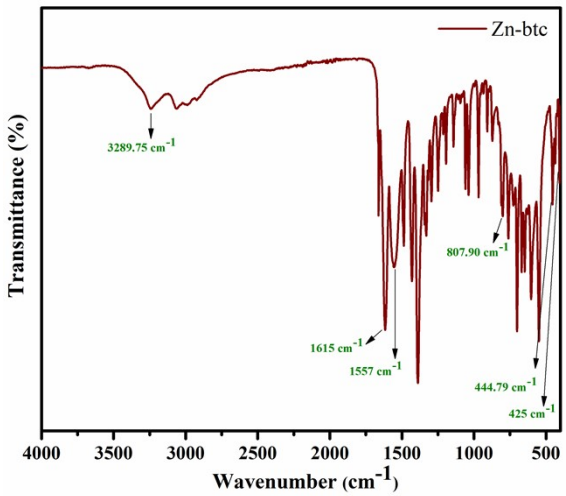

Figure S4: IR spectrum of Zn-btc: 3289.75 (N-H stretch),1615 (amide C=O stretch), 1557(amide II), 807.90 cm^{-1} (Zn-O symmetric stretching), 447.79 cm^{-1} (Zn-O symmetric stretching), 425 cm^{-1} (Zn-N symmetric stretching).

Section S6: XRPD Pattern of **Zn-cpb, Zn-bdc** and **Zn-btc**

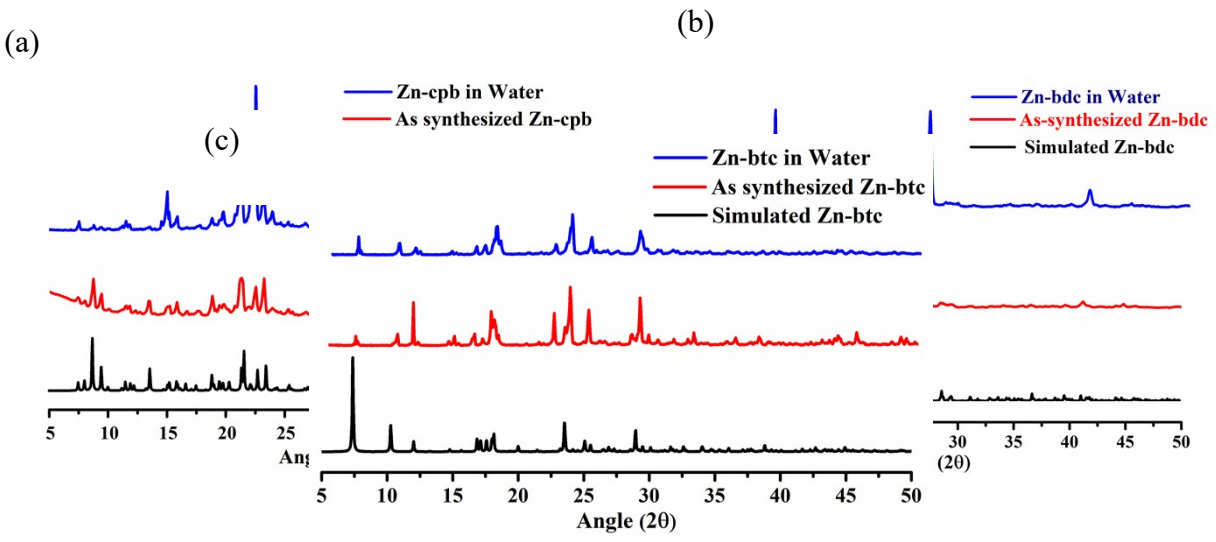

Figure S5. XRPD-pattern of MOFs to check its bulk purity as well as its aqueous stability (a) **Zn-cpb**, (b) **Zn-bdc**, (c) **Zn-btc**

Section S7: Thermogravimetric Analysis of **Zn-cpb, Zn-bdc** and **Zn-btc**

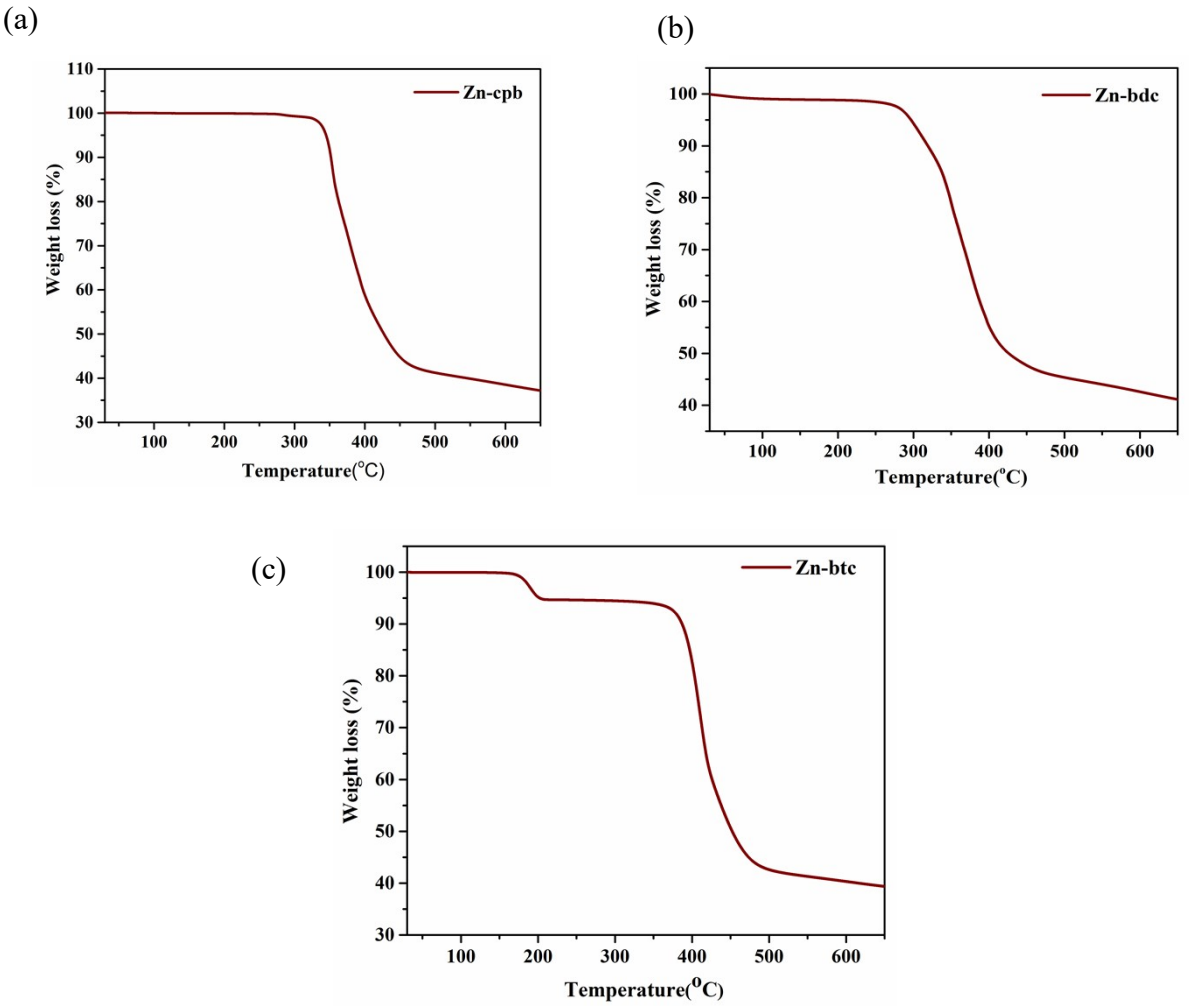

Figure S6. TGA of MOFs to check its thermal stability (a) **Zn-cpb**; (b) **Zn-bdc**, (c) **Zn-btc**

Section S8: UV-Visible spectral analysis.

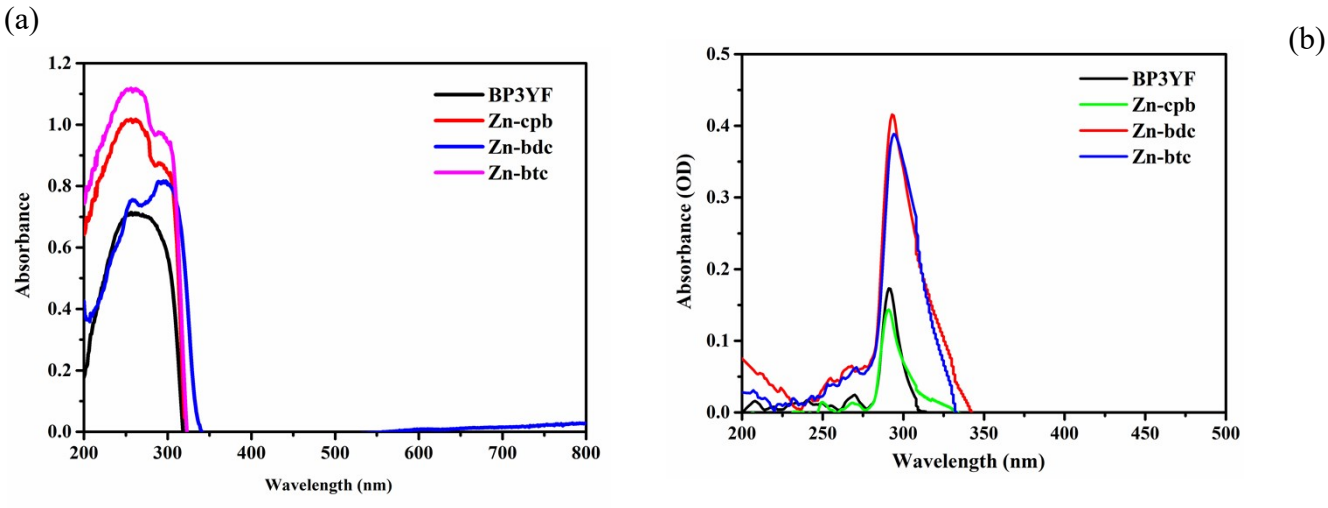

Figure S7. UV-visible absorbance spectra of MOFs in (a) solid state (b) dispersed phase.

Section S9: Photoluminescence (PL) study

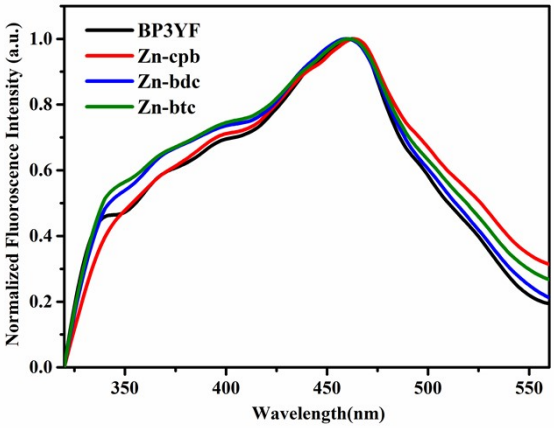

Figure S8. Solid-state emission spectra of ligand and MOFs.

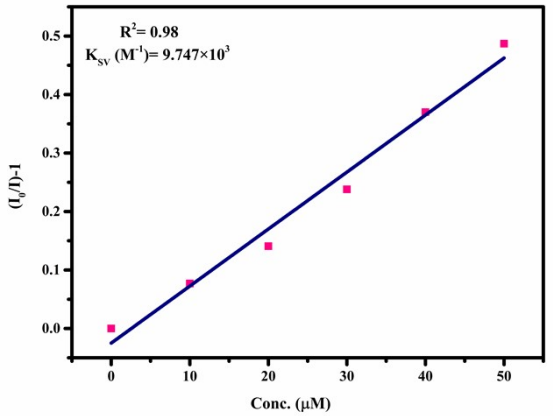

Figure S9. S-V plot of **Zn-bdc** for turn-off

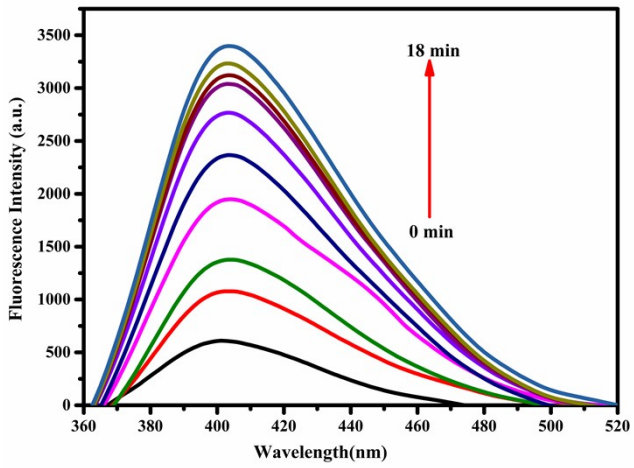

Figure S10 Time-dependent fluorescence spectra of **Zn-bdc**.

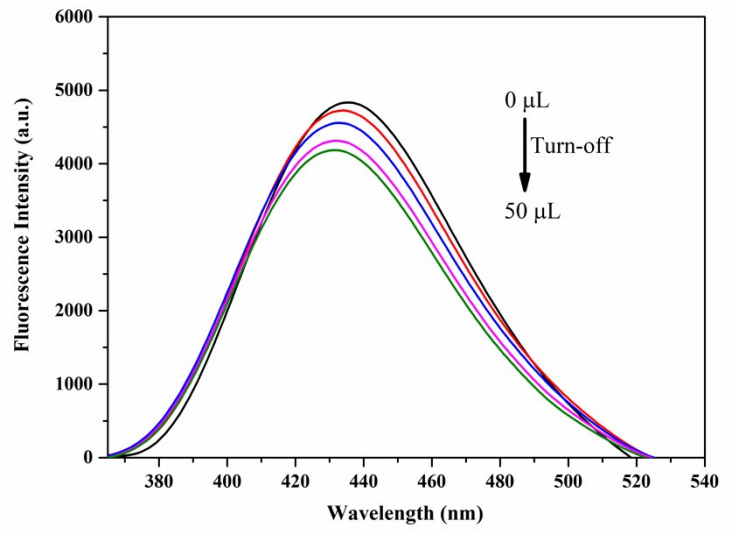

Figure S11. Concentration-dependent fluorescence turn-off response of **Zn-btc** upon addition of H_2S up to 50μL

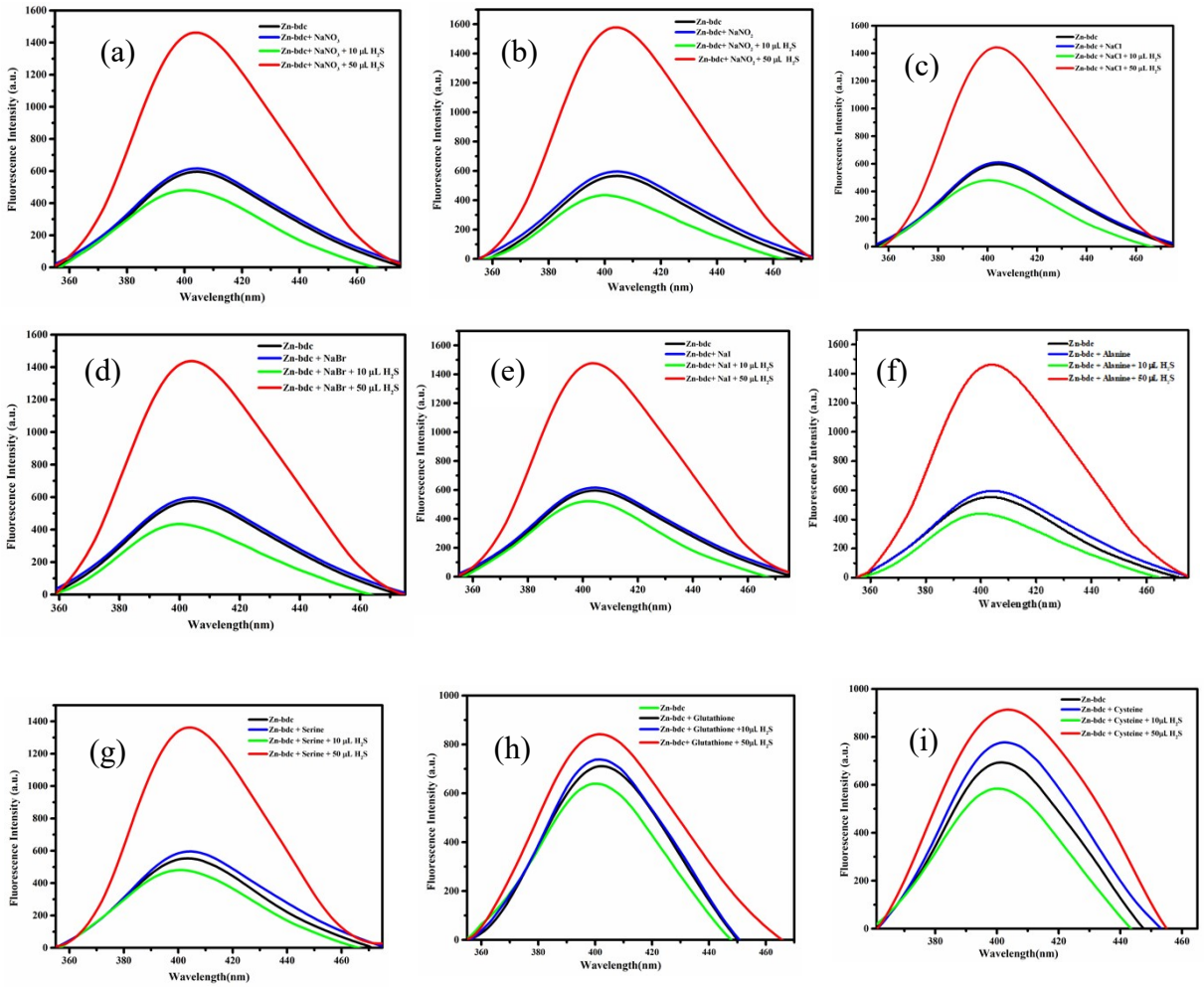

Figure S12. Fluorescence spectra upon addition of different analytes: (a)) $NaNO_3$; (b) $NaNO_2$ (c) NaCl; (d) NaBr; (e) NaI; (f) Alanine; (g) Serine; (h). Glutathione; (i) Cysteine

Section S10: Characterization of H_2S-treated material

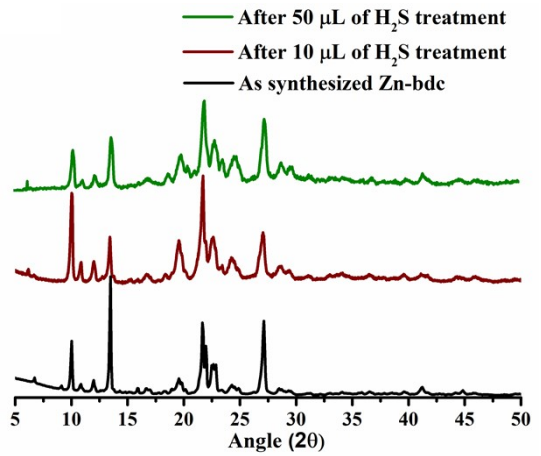

Figure S13. XRPD-pattern of **Zn-bdc** before and after performing H_2S treatment

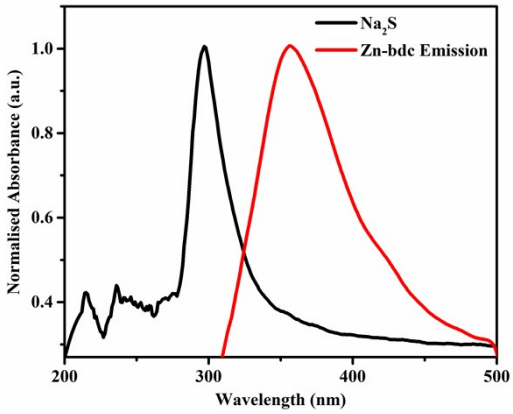

Figure S14. The UV-vis absorption of Na_2S and emission spectrum of **Zn-bdc.**

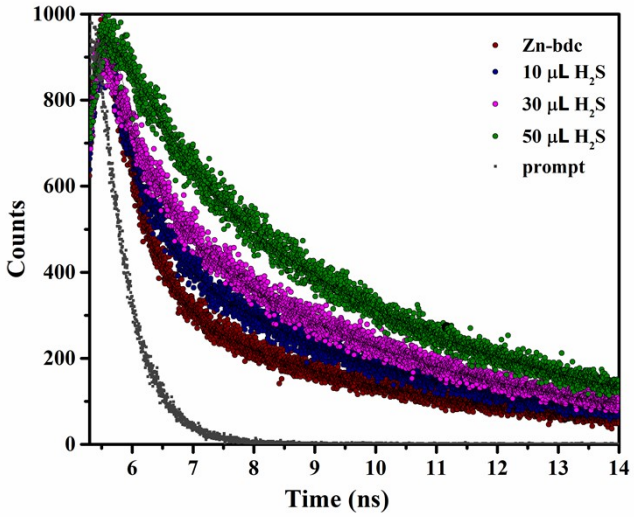

Figure S15. Fluorescence lifetime decay profile of **Zn-bdc** with incremental addition of H_2S

Table S3

Fluorescence lifetime data for **Zn-bdc** with H_2S

Amount added	τ_1 [ns]	α_1	τ_2 [ns]	α_2	τ_{av} [ns]
0 equiv.	0.085	0.96	4.08	0.04	0.24
0.5 equiv.	0.084	0.94	4.07	0.06	0.32
1.5 equiv.	0.18	0.84	4.2	0.16	0.82
2.9 equiv.	0.39	0.56	4.28	0.44	2.10

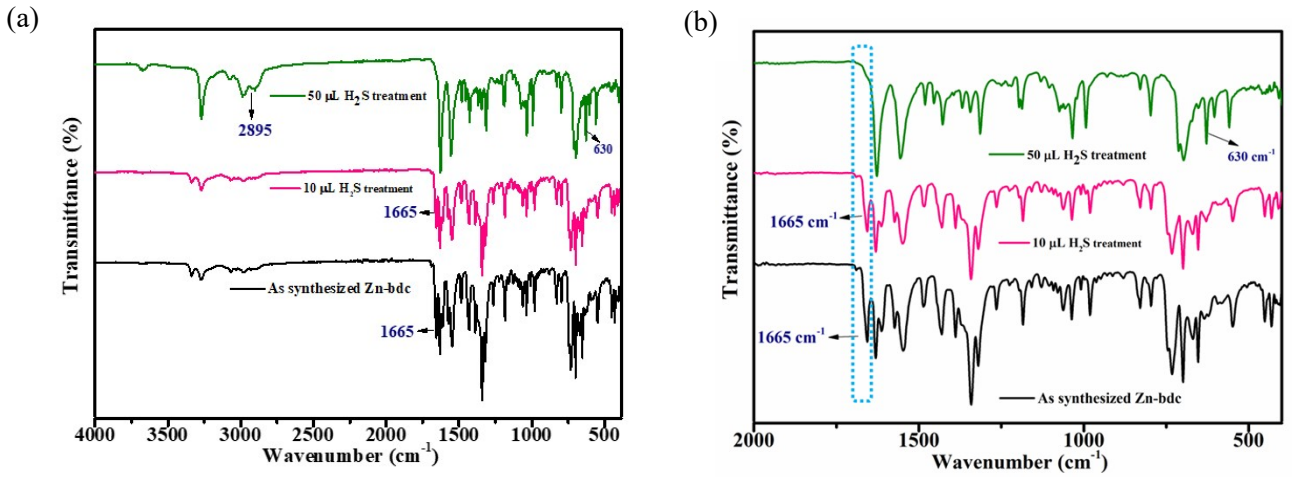

Figure S16. (a) FT-IR spectra of **Zn-bdc** before and after treatment with H_2S. (b) Enlarge portion of FT-IR spectra of **Zn-bdc** before and after treatment with H_2S.

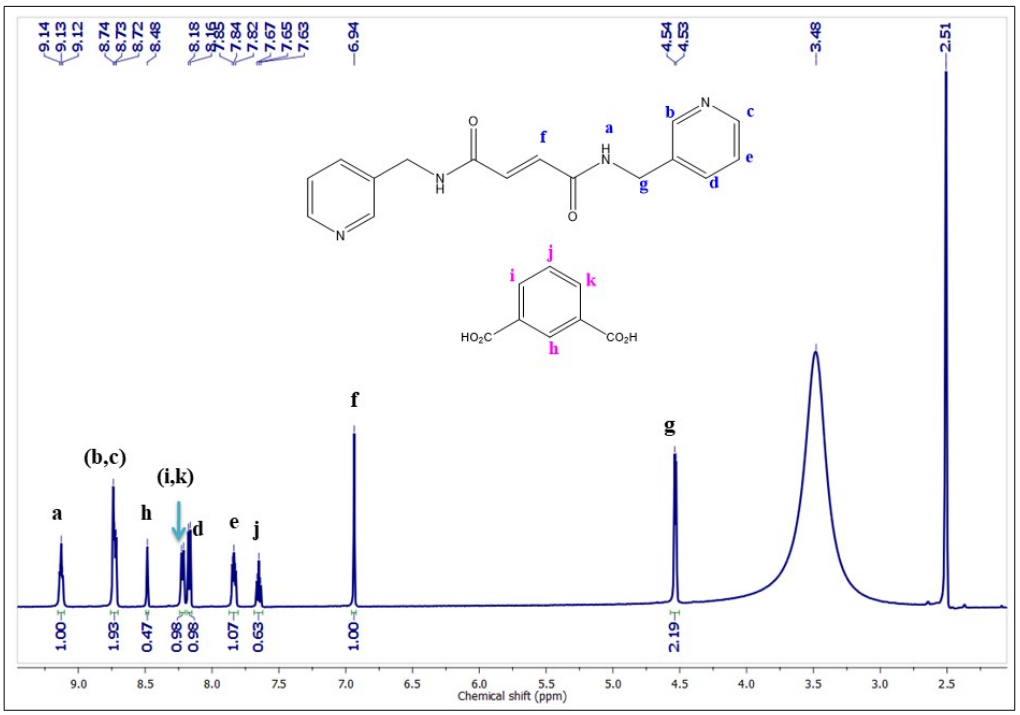

Figure S17. [1]H-NMR spectra of **Zn-bdc** in DMSO-d6 (digested with HCl).

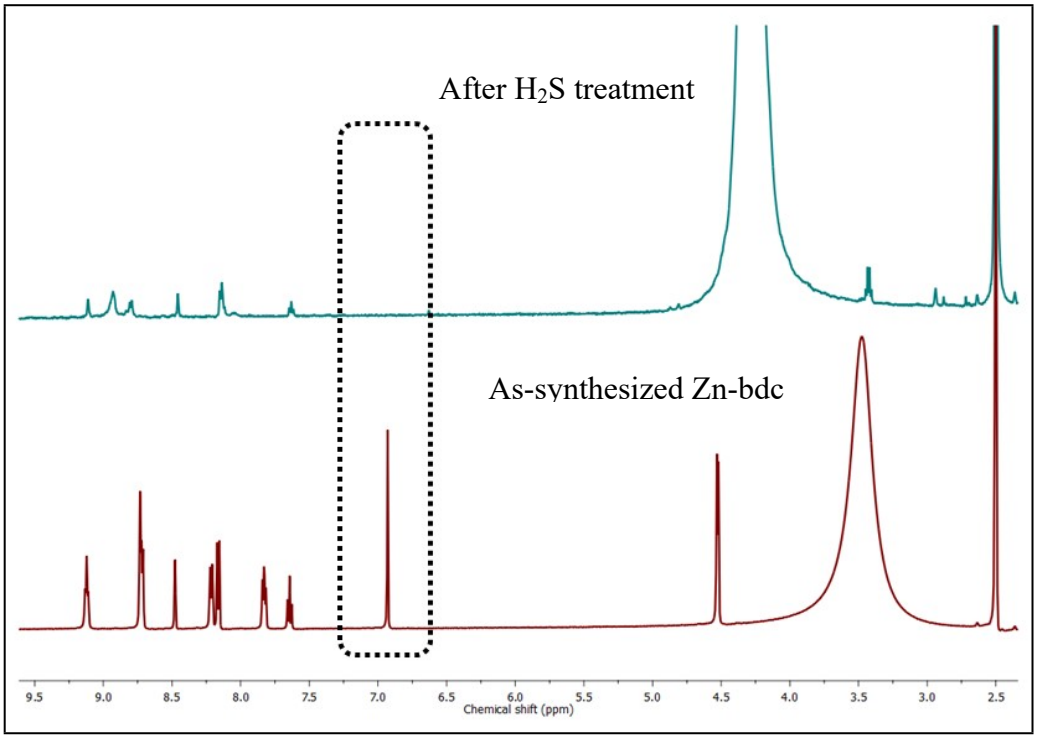

Figure S18. [1]H-NMR spectra of **Zn-bdc** before and after treating with H_2S in DMSO-d_6 (digested with HCl).

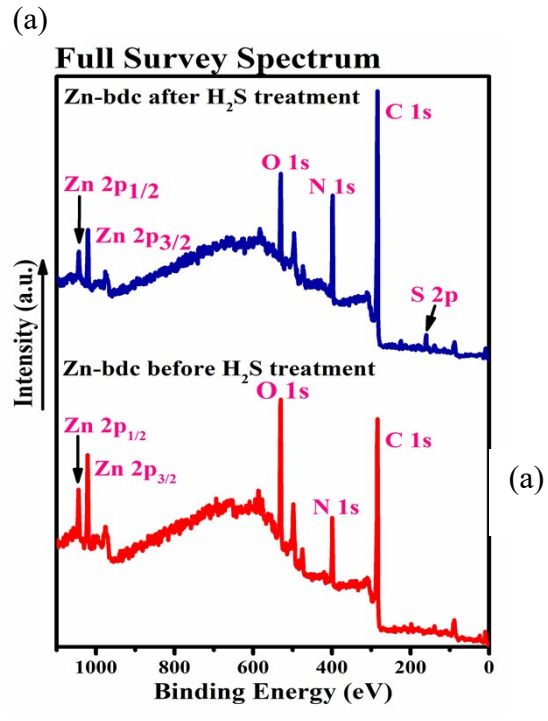
(a)
Full Survey Spectrum
Zn-bdc after H2S treatment
C 1s
O 1s
N 1s
Zn 2p1/2
Zn 2p3/2
S 2p
Zn-bdc before H2S treatment
O 1s
Zn 2p1/2
Zn 2p3/2
C 1s
N 1s
Intensity (a.u.)
1000 800 600 400 200 0
Binding Energy (eV)
(a)

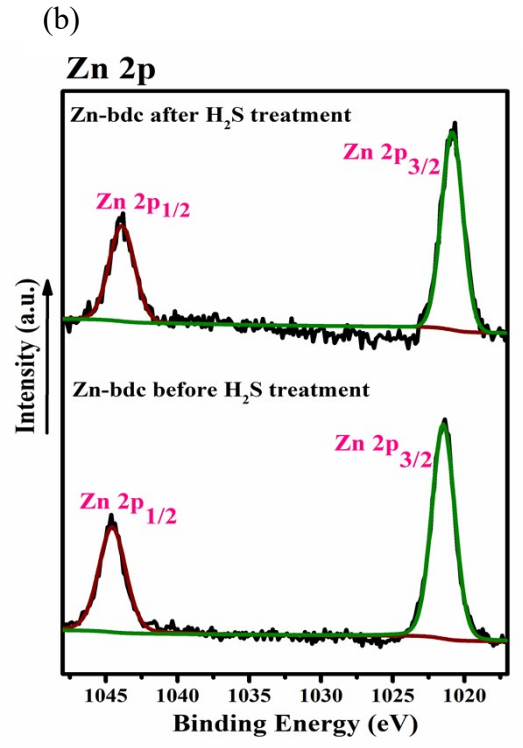
(b)
Zn 2p
Zn-bdc after H2S treatment
Zn 2p3/2
Zn 2p1/2
Zn-bdc before H2S treatment
Zn 2p3/2
Zn 2p1/2
Intensity (a.u.)
1045 1040 1035 1030 1025 1020
Binding Energy (eV)

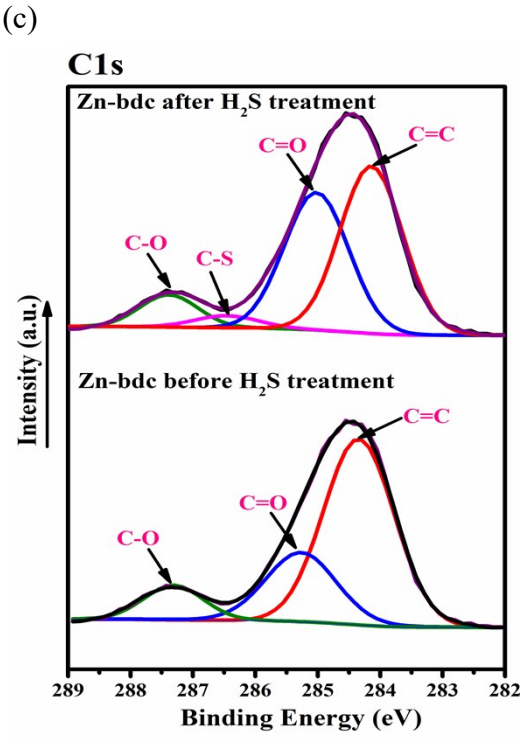
(c)
C1s
Zn-bdc after H2S treatment
C=O
C=C
C-O
C-S
Zn-bdc before H2S treatment
C=C
C=O
C-O
Intensity (a.u.)
289 288 287 286 285 284 283 282
Binding Energy (eV)

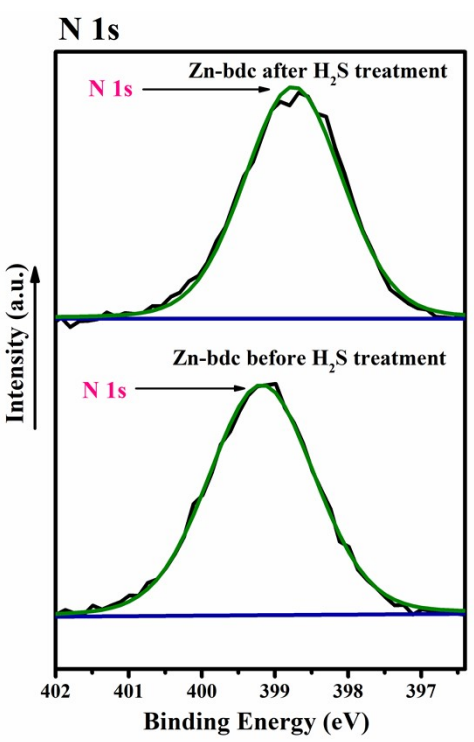
(d)
N 1s
Zn-bdc after H2S treatment
N 1s
Zn-bdc before H2S treatment
N 1s
Intensity (a.u.)
402 401 400 399 398 397
Binding Energy (eV)

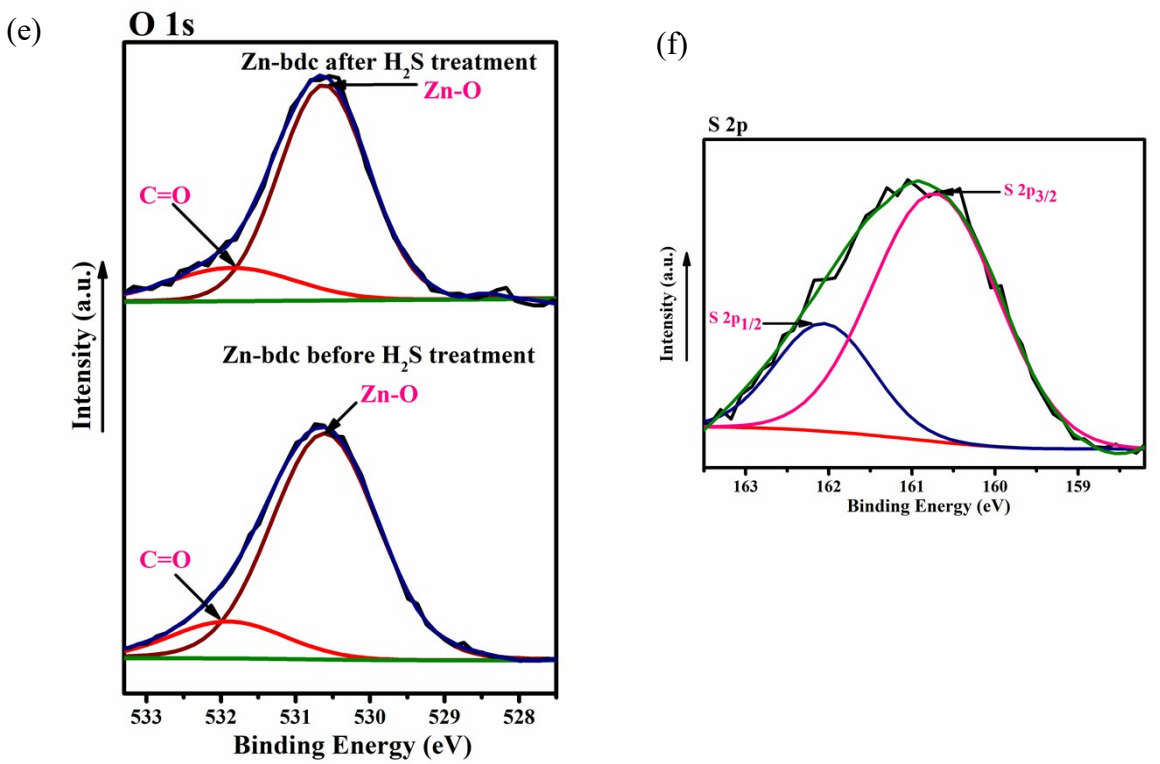

Figure S19. High-resolution XPS spectra of **Zn-bdc** before and after the addition of H_2S; (a) full survey spectrum, (b) Zn 2p, (c) C 1s, (d) N1S (e) O1S and (f) S 2p for **Zn-bdc** after the addition of H_2S.

Section S11: Real water specimen investigation

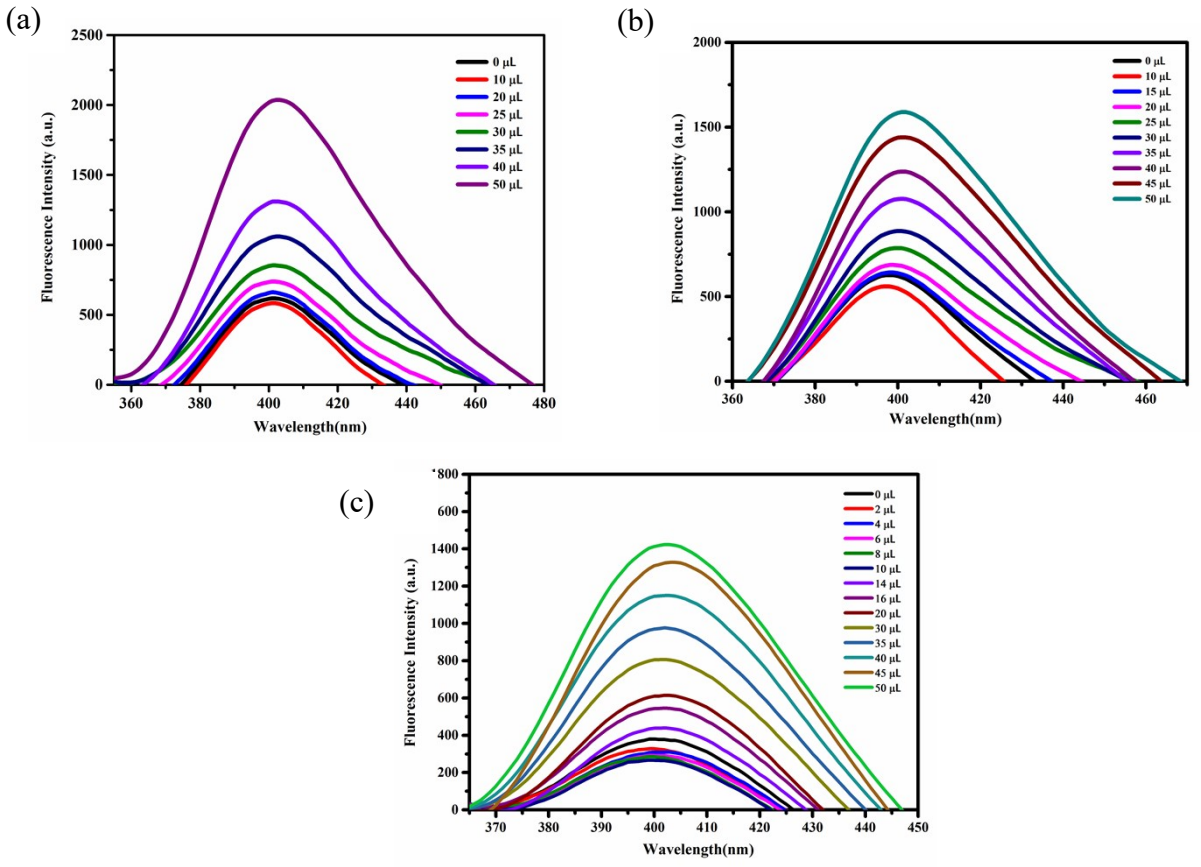

Figure S20. Change of the luminescence intensity spectra of **Zn-bdc** before and after the addition of H_2S in (a) Tap water (b) Lake water (c) River water

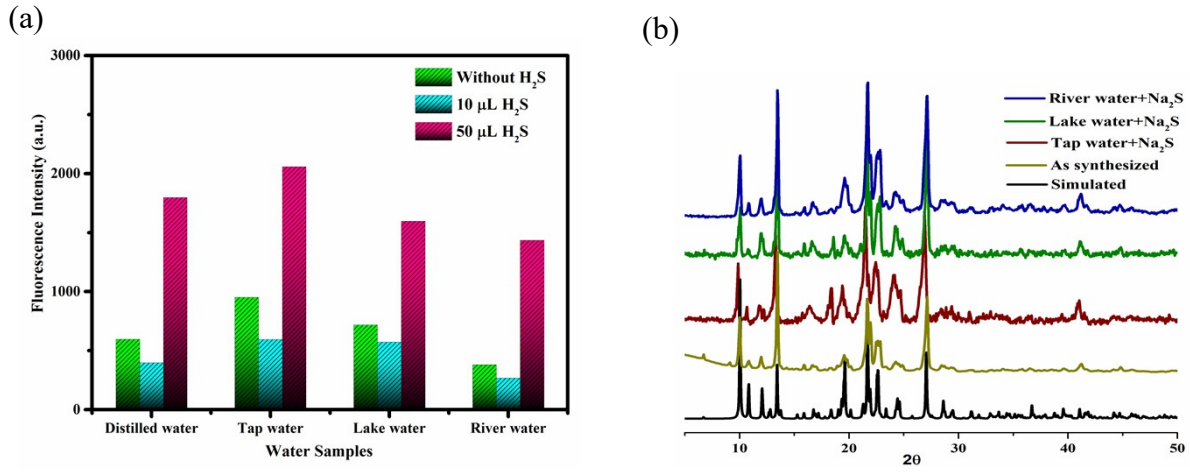

Figure S21. (a) Change of the luminescence intensity spectra of Zn-bdc in various water specimens before and after the addition of H_2S.(b) XRPD pattern of Zn-bdc in tap water, lake water, and river water after the addition of H_2S

Section S12. Gaseous phase H_2S detection in powder form

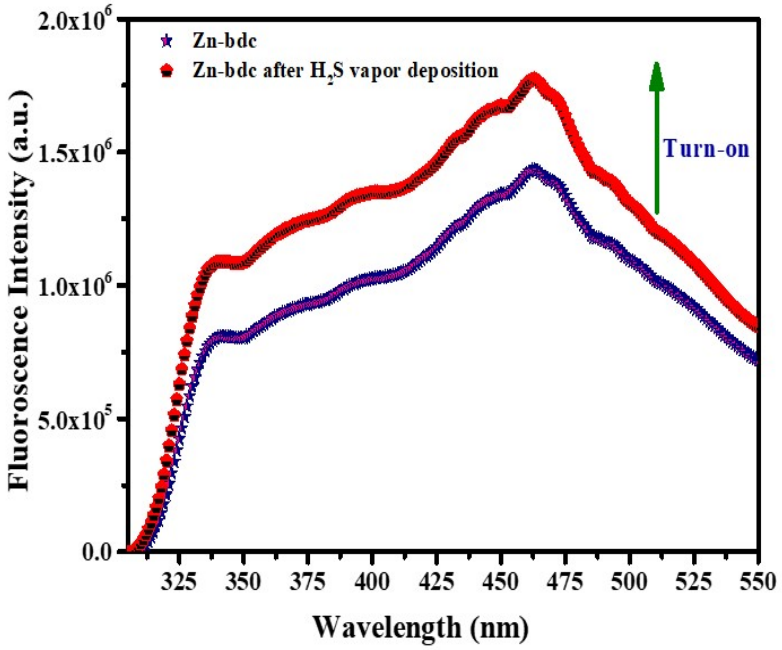

Figure S22. Change of the luminescence intensity spectra of Zn-bdc (a) before and after H_2S vapor deposition in powder of Zn-bdc

<u>Section S13</u> Fluorescence spectra of MOF-loaded composite membrane

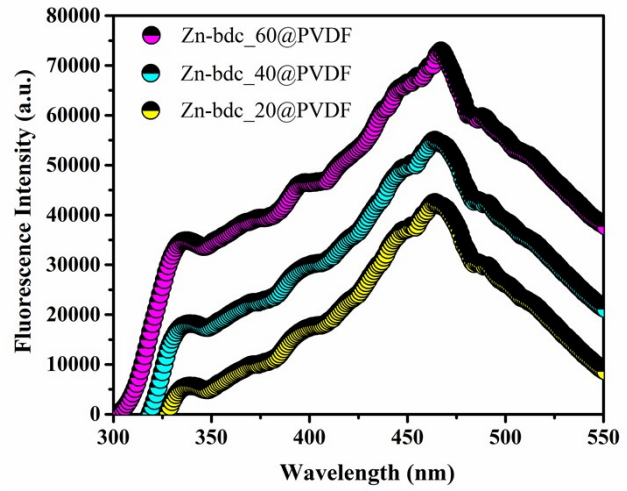

Figure S23. Change of the luminescence intensity spectra of Zn-bdc

Section S14 Effect of H_2S on the ligand

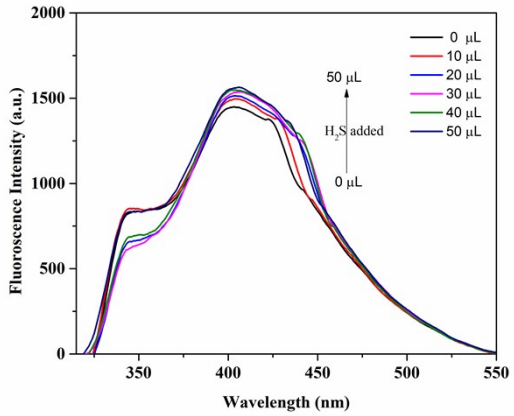

Figure S24. Titration of ligand BP3YF with H_2S

Section S15 . Colorimetric response of the MOF and its thin-film toward the H_2S study

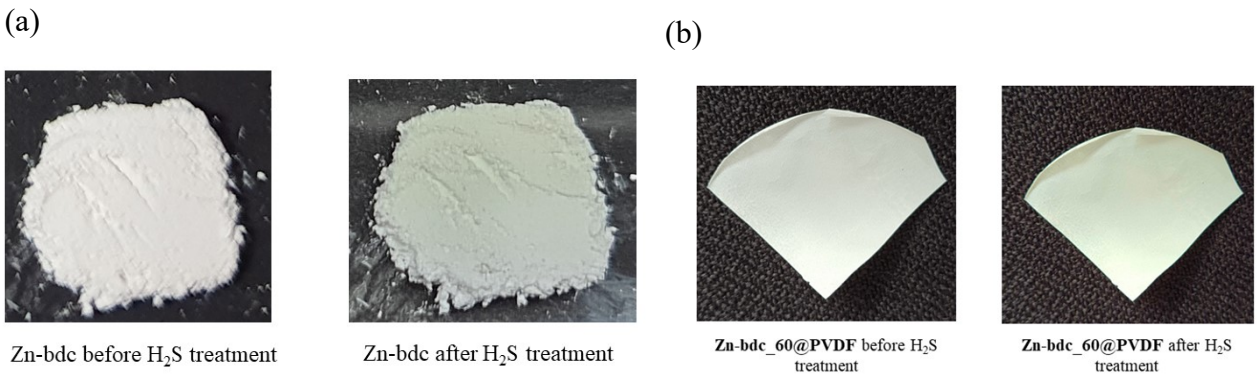

Figure S25. (a) colorimetric response of Zn-bdc MOF before and after H_2S treatment; (b) colorimetric response of Zn-bdc_60@PVDF before and after H_2S treatment

Section S16: Geometrical parameters of hydrogen bonds

Table S4

Complex	Types	Donor (D)	Acceptor (A)	H···A (Å)	D···A (Å)	D-H···A (°)
Zn-cpb	N-H···O	N4 N2	O6 O2	2.00 1.98	2.816 (9) 2.826 (9)	159 170
	C-H···O	C7 C15 C16 C19 C23 C25 C26 C28	07 O5 O5 O8 O5 O2 O6 O7	2.46 2.55 2.45 2.42 2.41 2.46 2.36 2.40	3.154 (10) 3.226 (11) 3.325 (10) 3.018 (9) 3.030 (9) 3.317 (10) 3.216 (11) 2.806 (10)	132 130 156 122 124 153 152 105
	C-H···N	C23	N4	2.49	2.854 (10)	103
Zn-bdc	N-H···O	N3 N4 N7 N10	O2 O7 O1 O6	2.30 2.07 2.12 2.27	3.15 (3) 2.93 (3) 2.98 (3) 3.14 (2)	177 176 171 177
	C-H···O	C10 C11 C14 C18 C19 C21 C23 C24 C28 C30 C34 C38 C39 C39 C42 C44 C45 C46 C47	O9 O1 O9 O1 O16 O10 O7 O3 O9 O8 O3 O7 O15 O10 O10 O5 O16 O15 O5	2.30 2.44 2.37 2.51 2.39 2.11 2.49 2.29 2.50 2.47 2.36 2.49 2.11 2.58 2.42 2.38 2.47 2.24 2.43	3.10 (2) 3.18 (3) 3.18 (2) 3.25 (3) 3.32 (4) 3.07 (4) 3.22 (3) 3.09 (2) 2.81 (2) 2.79 (2) 3.16 (3) 3.22 (3) 3.08 (4) 2.91 (4) 2.80 (4) 3.31 (4) 2.78 (3) 2.59 (5) 2.74 (3)	143 136 146 137 159 168 136 143 100 100 144 136 174 100 104 161 100 102 100
	C-H···N	C13 C14 C34 C49	N3 N4 N7 N10	2.52 2.56 2.49 2.53	2.83 (4) 2.91 (3) 2.86 (3) 2.84 (4)	100 103 103 100
Zn-btc	N-H···O	N2	O4	1.92	2.827 (5)	155
	C-H···O	C1 C4 C6	O6 O1 O1	2.41 2.60 2.40	3.048 (6) 3.432 (7) 2.813 (6)	125 150 105

Section S17. Cytotoxicity assay analysis

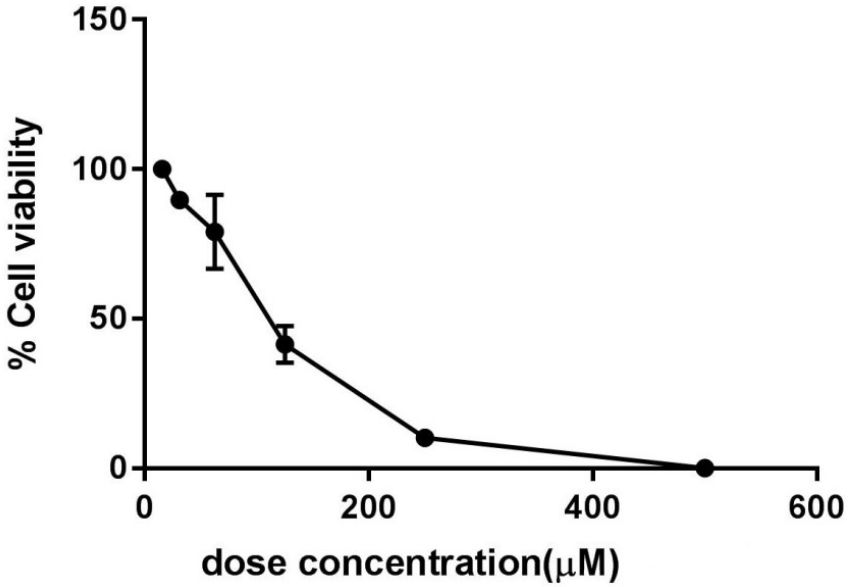

Figure S26. Cytotoxicity assay analysis of **Zn-bdc**

Section S15:

Comparison of the various existing MOFs for the sensing of H_2S in solution phase

Table S5

Entry	MOF used	Detection process	Response time(sec)	Detection limit	Sensing medium	Analyte	Ref.
1	Eu-BDC−CH=CH_2		<120	38.4 μM	HEPES buffer	NaHS	S2
2	CP-1 {[Zn(4-bmpbd)(AIP)].2H_2O}$_n$	Fluorescence 'turn-on'	30	7.2 μM	Water	Na_2S	S3
3	Al-MIL-53-NO_2	Fluorescence 'turn-on'	-	69.3 μM	Water	NaHS	S4
4	CAU-10-V-H	Fluorescence 'turn-off'	10	1.65 μM	HEPES buffer	NaHS	S5
5	Cu^{2+}/Eu^{3+}/TFA@MIL-140C	Fluorescence 'turn-on'	30	7.43 μM	HEPES buffer	NaHS	S6
6	Al-MIL-53-N_3	Fluorescence 'turn-on'	180	0.09 μM	HEPES buffer	Na_2S	S7

7	UiO-66-$(NO_2)_2$	Fluorescence 'turn-on'	2400	14.14 µM	HEPES buffer	Na_2S	S8
8	Tb^{3+}@Cu1 Cu1=$[Cu(HCPOC)_2]_n$	Fluorescence 'turn-on'	120	1.2 µM	HEPES buffer	Na_2S	S9
9	UiO-66-$CH=CH_2$	Fluorescence 'turn-off'	10	6.46 µM	HEPES buffer	NaHS	S10
10	$[Zn(L)(4,4'\text{-}bpy)_{0.5}](H_2O)_{0.25}$	Fluorescence 'turn-off'	150	7.9 µM	Water	Na_2S	S11
11	$[Cd_4(L)_4(4,4'\text{-}bpy)_2](H_2O)_{0.25}$	Fluorescence 'turn-off	65	0.2 µM	Water	Na_2S	S11
12	CAU-10-N_3	Fluorescence 'turn-on'	900	2.65 µM	HEPES buffer	Na_2S	S12
13	DUT-52-$(NO_2)_2$	Fluorescence 'turn-on'	3300	20 µM	HEPES buffer	Na_2S	S13
14	$Eu^{3+/}Cu^{2+}$@UiO-66-(COOH)	Fluorescence 'turn-on'	30	5.45 µM	HEPES buffer	NaHS	S14
15	Ce-UiO-66-N_3	Fluorescence 'turn-on'	760	12.2 µM	HEPES buffer	NaHS	S15
16	Ce-UiO-66-NO_2	Fluorescence 'turn-on'	760	34.8 µM	HEPES buffer	NaHS	S15
17	Fe^{III}-MIL-88-NH_2	Fluorescence 'turn-on'	-	Fluorescence 'turn-on'	Water	NaHS	S16
18	Al-MIL-101-N_3	Fluorescence 'turn-on'	120	100 nm	Water	Na_2S	S17
19	IRMOF-3(–N_3)	Fluorescence 'turn-on'	90	28.3 µM	HEPES buffer	Na_2S	S18
20	Zr-UiO-66-NO_2	Fluorescence 'turn-on'	460	188 µM	HEPES buffer	Na_2S	S19
21	Zr-UiO-66-N_3	Fluorescence 'turn-on'	180	118 µM	HEPES buffer	Na_2S	S20
22	CD-MONT-2'	Fluorescence 'turn-on'	900	0.058 µM	PBS buffer+ 1%DMSO	Na_2S	S21
23	$\{CuL[AlOH]_2\}_n$	Fluorescence 'turn-on'	-	16 nM	BBS butter	NaHS	S22
24	MN-ZIF-90	Fluorescence 'turn-on'	-	Not specified	Water	H_2S solution	S23
25	BFMOF-1	Colorimetric analysis	1800	17.6 µM	Water	H_2S solution	S24
26	TP-MOF	Fluorescence 'turn-on'	3600	26.6 µM	HEPES buffer	NaHS	S25
27	Eu^{3+}/Ag^{+}@UiO-66-	Fluorescence	30	23.53	HEPES	NaHS	S26

	$(COOH)_2$	Turn-off		µM	buffer		
28	UiO-66-NN-BQB	Fluorescence 'turn-on'	18000	1.74 µM	Water	H_2S solution	S27
29	Fe_xAl_{1-X} MIL	Fluorescence 'turn-on'	90	4.69 µM	Water	NaHS	S28
30	Cu-HIA	Fluorescence 'turn-on'	30	0.21 µM	Water	Na_2S	S29
31	$Eu^{3+/}Cu^{2+}$@Znpda	Fluorescence 'turn-on'	60	1.45 µM	HEPES	NaHS	S30
32	DUT-52-N_3	Fluorescence 'turn-on'	120	0.5 µM	HEPES	Na_2S	S31
33	UiO-66-NO_2	Fluorescence 'turn-on'	<120	5.128 µM	HEPES	Na_2S	S32
33	**Zn-bdc** $\{[Zn_2(BP3YF)_2(bdca)_2]\}_n$	Fluorescence 'turn-off' and 'turn-on'	9	15.3 µM and 10.7 µM	Water	Na_2S	This work

Comparison of the various existing MOFs based mixed-matrix membrane by PVDF for the sensing of H_2S

Table S6

Entry	**MOF used**	**Type of material**	**Detection process**	**Detection limit**	**Sensing medium**	**Reaction strategies**	**Ref.**
1.	Zn-bdc_60@PVDF	Mixed-matrix membrane	fluorescence 'turn-on'	5.3 µM	Gas	Nucleophilic addition reaction	This work
2.	Al-MIL-53-NO_2 MMM (70 wt%)	MOF MMM	fluorescence 'turn-on'	92.31 nM	Gas	Reductive reaction	S33

References:

S1. L. Rajput, S. Singha and K. Biradha, *Cryst. Growth Des.,* 2007, **7**, 2788.

S2. X. Han, J. Liu, K. Yu, Y. Lu, W. Xiang, D. Zhao and Y. He, *Inorg. Chem.,* 2022, **61**, 5067.

S3. S. Saha, P. K. Roy, K. Maity, M. Mandal and K. Biradha, *Chem. Eur. J.,* 2021, **28**, e202103830.

S4. Z. Zhu, X. He and W. –N. Wang, *CrystEngComm.,* 2020, **22**, 195.

S5. S. Nandi, H. Reinsch and S. Biswas, *Microporous and Mesoporous Materials.,* 2020, **293**, 109790.

S6. Z. Wang, X. Wang, J. Li, W. Li and G. Li,. *Journal of Inorganic and Organometallic Polymers and Materials.,* 2019, **29**, 2124.

S7. A. Das, S. Banesh, V. Trivedi and S. Biswas, *Dalton Trans.,* 2018, **47**, 2690.

S8. S. Nandi, S. Banesh, V. Trivedi and S. Biswas, *Analyst.* 2018, **143**, 1482.

S9. X. Zheng, R. Fan, Y. Song, A. Wang, K. Xing, X. Du, P. Wang and Y. Yang, *J. Mater. Chem. C.* **2017**, *5*, 9943.

S10. Y. Li, X. Zhang, L. Zhang, K. Jiang, Y. Cui, Y. Yang and G. Qian, *Journal of Solid state Chemistry.* 2017, **255**, 97.

S11. X. –F. Yang, H. –B. Zhu and M. Liu, *Inorganic Chimica Acta.,* 2017, **466**, 410.

S12. S. Nandi, H. Reinsch, S. Banesh, N. Stock, V. Trivedi and S. Biswas, *Dalton Trans.,* 2017, **46**, 12856.

S13. R. Dalapati, S. N. Balaji, V. Trivedi, L. Khamari, S. Biswas, *Sensors and Actuators B.,* 2017, **245**, 1039.

S14. X. Zhang, Q. Hu, T. Xia, J. Zhang, Y. Yang, Y. Cui, B. Chen and G. Qian, *ACS Appl. Mater. Interfaces.,* 2016, **8**, 32259.

S15. A. Buragohain and S. Biswas, *CrystEngComm.,* 2016, **18**, 4374.

S16. Y. –Y. Cao, X. –F. Guo and H. Wang, *Sensors and Actuators B.,* 2017, **243**, 8.

S17. A. Legrand, A. Pastushenko, V. Lysenko, A. Geloen, E. A. Quadrelli, J. Canivet and D. Farrusseng, *ChemNanoMat.,* 2016, **2**, 866.

S18. X. Zhang, J. Zhang, Q. Hu, Y. Cui, Y. Yang and G. Qian, *Applied Surface Science.,* 2015, **355**, 814.

S19. S. S. Nagarkar, A. V. Desai, S. K. Ghosh, *Chem. Eur. J.,* 2015, **21**, 9994.

S20. S. S. Nagarkar, T. Saha, A. V. Desai, P. Talukdar and S. K. Ghosh, *Sci. Rep.,* 2014, **4**, 7053.

S21. X. Xin, J. Wang, C. Gong, H. Xu, R. Wang, S. Ji, H. Dong, Q. Meng, L. Zhang, F. Dai and D. Sun, *Sci. Rep.,* 2016, **6**, 21951.

S22. Y. Ma, H. Su, X. Kuang, X. Li, T. Zhang and B. Tang, *Anal. Chem.,* 2014, **86**, 11459.

S23. H. Li, X. Feng, Y. Guo, D. Chen, R. Lui, X. Ren, X. Jiang, Y. Dong and B. Wang, *Sci. Rep.,* 2014, **4**, 4366.

S24. J. Cui, Y. –L. Wong, M. Zeller, A. D. Hunter and Z. Xu, *Angew. Chem. Int. Ed.,* 2014, **53**, 14438.

S25. C. Yang, K. Chen, M. Chen, X. Hu, S. –Y. Huan, L. Chen, G. Song and X. –B. Zhang, *Anal. Chem.,* 2019, **91**, 2727.

S26. X. Zhang, L. Fang, K. Jiang, H. He, Y. Yang, Y. Cui, B. Li and G. Qian, *Biosensors And Bioelectronics.,* 2019, **130**, 65.

S27. H. Yu, C. Liu, Y. Li and A. Huang, *ACS Appl. Mater. Interfaces* **2019**, *11*, 41972-41978.

S28. Z. Zhu, V. Natarajan and W. –N. Wang, *Journal of Solid state Chemistry.,* 2020, **288**, 121434.

S29. X. Zhao, L. Zhang, J. Bai, P. Wu, Y. Li, L. Liang, L. Xie and J. Wang, *Spectrochimica Acta Part A: Molecular and Biomolecular Spectroscopy.,* 2020, **243**, 118794.

S30. X. Han, C. Gu, Y. Ding, J. Yu, K. Li, D. Zhao and B. Chen, *ACS Appl. Mater. Interfaces.,* 2021, **13**, 20371.

S31. C. Gogoi, A. Kumar, M. SK, S. Biswas, *Microporous and Mesoporous Materials.,* 2021, **311**, 110725.

S32. K. Yu, Q. Wang, Z. Li, Z. Xin, X. Han, T. Alshahrani, Y. He, D. Zhao and B. Chen, *Microporous and Mesoporous Materials.*, 2023, **356**, 112594.

S33. X. Zhang, Q. Zhang, D. Yue, J. Zhang, J. Wang, B. Li, Y. Yang, Y. Cui and G. Qian, *Small*., 2018, 14, 1801563.